Progress In Electromagnetics Research B, Vol. 68, 73–88, 2016

Diffraction of Axially-Symmetric TM-Wave from Bi-Cone Formed by Finite and Semi-Infinite Shoulders

Dozyslav B. Kuryliak and Oleksiy M. Sharabura*

Abstract—The problem of axially-symmetric TM-wave diffraction from a perfectly conducting bi-cone is analyzed. Bi-cone is formed by finite and semi-infinite conical shoulders and illuminated by ring magnetic source. The problem is formulated in a spherical coordinate system as a mixed boundary problem for Helmholtz equation. The unknown H_φ-diffracted field is sought as expansion in series of eigenfunctions for each region, formed by the bi-cone. The solution of the problem then is reduced to the infinite set of linear algebraic equations (ISLAE) of the first kind by means of mode matching technique and orthogonality properties of the eigen functions. The main parts of the asymptotic expressions of ISLAE matrix elements, determined for large indexes, identify the convolution type operator. The corresponding inversed operator is represented in an explicit form. Two of these operators are applied to reduce the problem to the ISLAE of the second kind and to determine the new analytical regularization method for the solution of wave diffraction problems for bi-conical scatterers. The unknown expansion coefficients can be determined from the ISLAE with the given accuracy by the reduction method. The particular cases such as low frequency approximation and transition from bi-cone to conical monopole and disc-cone scatterer are analyzed. The numerically obtained results are applied to the analysis of scattering properties of hollow conical monopoles and disc-conical scatterers.

1. INTRODUCTION

Bi-conical antennas possess the broadband properties, provide an omnidirectional radiation, and their characteristics, which are necessary for signal transmission, can be achieved by the bi-conical structures of small size. Different types of bi-conic antennas are widely applied in modern communication technologies; they are also used for reference measurements and system verifications [1–7]. The use of bi-cones as the radiating elements in the radio communication started more than a century ago [8]. However, the in-depth study of bi-conical antennas was initiated only in the late 1930s. Earliest patents for bi-conical irradiators and antennas are given in [9, 10]. At the same time, the methods of theoretical analysis of electromagnetic fields interaction with the bi-conic scatterers started to develop. A convenient theoretical model of a bi-conical antenna was first introduced in [11]. Then in [12, 13], the problem of electromagnetic excitation of finite bi-cone was formulated rigorously by taking into account all the boundary conditions. To solve this problem, the field components were represented as a sum of normal modes of subdomains. The lowest TEM-mode, which is excited in the bi-conical area, causes the wide-band properties; it is also taken into account in the field representations. The orthogonality properties of normal waves were used to reduce the problem to the infinite system of linear algebraic equations (ISLAE) with the help of the mode-matching technique. Numerous papers were devoted to the problem of excitation of the bi-cones, using this idea. The focus was on the important particular cases of bi-conical structures such as finite symmetrical bi-cones formed by the closed conical shoulders [14, 15],

Received 13 April 2016, Accepted 13 May 2016, Scheduled 31 May 2016
* Corresponding author: Oleksiy M. Sharabura (shom@ipm.lviv.ua).
The authors are with the Department of Physical Bases of Materials Diagnostics, Karpenko Physico-Mechanical Institute of the NAS of Ukraine, Lviv 79060, Ukraine.

disc-conical structures [16], conical monopoles [17, 18] and the combinations of metal cones with spherical sectors [19, 20].

The early articles considered only the structures with wide [14, 17, 18] or narrow [15, 20] conical (bi-conical) regions, which allowed to simplify the analysis. Scattered characteristics of different bi-cones with numerous geometrical parameters obtained through mode-matching can be found in [21]. These works formed the classic theory of electromagnetic waves interaction with the perfectly conducting finite bi-cones based on the mode matching technique.

Kontorovich-Lebedev integral transformation and the semi-inversion technique were introduced in [22–24] for the analysis of wave diffraction from perfectly conducting bi-cones formed by semi-infinite and truncated cones. In [25] Kontorovich-Lebedev integral transformation and Wiener-Hopf method were applied to the analysis of the radially conducting finite bi-cones. In [26], this integral transformation and Riemann-Hilbert method were used for wave diffraction analysis of the radially slotted semi-infinite bi-cones.

The widespread use of bi-conical elements in different areas of modern physics and technology, including nanotechnologies [27, 28], requires a deep study of the physical properties of electromagnetic fields interaction with bi-conical structures. Contemporary theoretical studies of the scattering properties of the bi-cones are based on the mathematical modeling, which uses the direct numerical methods [1, 2] and the mode-matching technique in time domain [29] which is based on the Mode Basis Method [30].

We return to the problem of wave diffraction from bi-cones with the finite shoulder/s once again because the classic theory is based on the formalism of the mode-matching. The question of how to properly take into account the singularity of the field component normal to the edges is not answered by this theory. Also, the rules for reduction of ISLAE, which ensure obtaining the solutions in the required class of sequences, are unknown. Here we offer the analytical regularization method (semi-inversion method) to solve this diffraction problem. Our approach is based on the formulation of the mixed boundary diffraction problem and analytical inversion of the singular part of the appropriate operator. This approach provides effective algorithms for diffracted field calculations to satisfy all the necessary conditions. The idea of analytical regularization was applied to the analysis of wave diffraction from waveguide discontinuities in [31]. Our technique was earlier applied to the analysis of wave diffraction on the conical (bi-conical) structures in [32–35].

2. STATEMENT OF THE PROBLEM

Let us consider the perfectly conducting bi-conical surface $Q = Q_1 \bigcup Q_2$ in spherical coordinate system (r, θ, φ), where $Q_1 : \{r \in (0, \infty), \theta = \gamma_1; \varphi \in [0, 2\pi)\}$ and $Q_2 : \{r \in (0, a_1), \theta = \gamma_2; \varphi \in [0, 2\pi)\}$ are the semi-infinite and finite hollow cones respectively with $\gamma_2 > \gamma_1$ and $\gamma_{1(2)} \neq \pi/2$ (see Fig. 1).

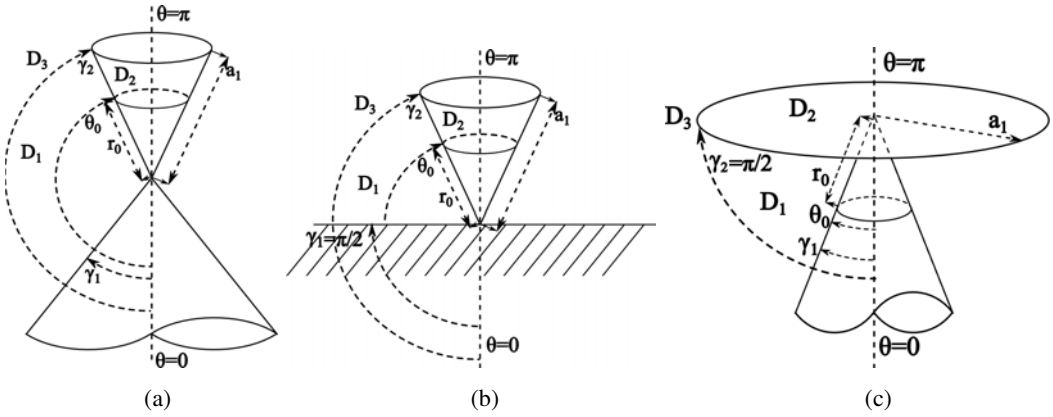

Figure 1. Geometrical scheme; (a) semi-infinity bi-cone; (b) conical monopole; (c) disc-conical antenna.

Let bi-cone Q be excited by the ring source with magnetic current density $\vec{J}(0,0,-J_\varphi)$, where

$$J_\varphi(r,\theta)=\frac{I_\varphi^{(m)}(r_0,\theta_0)}{r_0\sin\theta_0}\delta(r-r_0)\delta(\theta-\theta_0), \tag{1}$$

where $I_\phi^{(m)}$ is the magnetic current, $\delta(\ldots)$ the Dirac delta function, and r_0,θ_0 are source spherical coordinates, $0<r_0<a_1$, $\gamma_1\le\theta_0\le\gamma_2$. Time factor $e^{-i\omega t}$ is suppressed throughout this paper.

Since $I_\varphi^{(m)}$ is symmetrical and independent azimuth angle φ then, following from Maxwell equations, the source in Equation (1) excites three nonzero axially symmetric field components $E_r, E_\theta, H_\varphi(r,\theta)$, and the electric field is expressed in terms of H_φ by

$$\begin{aligned} E_r&=-\frac{1}{i\omega\varepsilon}\frac{1}{r\sin\theta}\frac{\partial}{\partial\theta}(\sin\theta H_\varphi),\\ E_\theta&=\frac{1}{i\omega\varepsilon}\frac{1}{r}\frac{\partial}{\partial r}(rH_\varphi). \end{aligned} \tag{2}$$

Here ε is the dielectric permittivity of the medium. Taking into account the axial symmetry of the initial problem, let us formulate the mixed value boundary problem to determine H_φ-field diffracted from Q as

$$\Delta H_\varphi-\frac{H_\varphi}{r^2\sin^2\theta}+k^2H_\varphi=0, \tag{3}$$

where $k=\omega\sqrt{\varepsilon\mu}$ is the wave number, $k=k'+\mathrm{i}k''$, $k',k''>0$; μ is the magnetic permeability; Δ is the Laplace operator,

$$\Delta=\frac{\partial^2}{\partial r^2}+\frac{2}{r}\frac{\partial}{\partial r}+\frac{1}{r^2\sin\theta}\frac{\partial}{\partial\theta}\left(\sin\theta\frac{\partial}{\partial\theta}\right).$$

The unknown H_φ-field satisfies the boundary condition at Q as

$$\frac{1}{\sin\theta}\frac{\partial}{\partial\theta}\left[\sin\theta(H_\varphi+H_\varphi^i)\right]_{r,\theta\in Q}=0, \tag{4}$$

where H_φ^i is the known magnetic component of the incident field produced by the source in Equation (1). We search for the solution of the mixed value boundary problem in Equations (3), (4) in class of functions that satisfy the Silver-Muller radiation condition in form

$$\lim_{r\to\infty}r\left[\vec{i}_r\times\vec{H}+Z^{-1}\vec{E}\right]=0, \tag{5}$$

where $Z=\sqrt{\mu/\varepsilon}$ is the medium wave resister, as well as energy limitation condition as

$$\int\limits_V\left(\varepsilon|\vec{E}|^2+\mu|\vec{H}|^2\right)dv<\infty. \tag{6}$$

Here V is any finite volume of integration. To determine the incident field $H_\varphi^i(r,\theta)$, we solve the auxiliary problem of semi-infinite bi-cone Q^∞ excitation by the ring source in Equation (1), where $Q^\infty=Q_1^\infty\bigcup Q_2^\infty$ and $Q_l^\infty=\{r\in[0,\infty),\,\theta=\gamma_l,\,\varphi\in[0,2\pi)\}$, $l=1,2$. Using the field representation as superposition of elementary bi-conical harmonics, we find that

$$H_\varphi^i(r,\theta)=\frac{i\omega\varepsilon}{\sqrt{\rho}}\sum_{n=1}^{\infty}B_n\Psi_{\nu_n-1/2}(\cos\theta)\begin{cases}K_{\nu_n}(\rho)I_{\nu_n}(\rho_0),\ r\ge r_0,\\ I_{\nu_n}(\rho)K_{\nu_n}(\rho_0),\ r\le r_0.\end{cases}\quad 0\le r<\infty,\ \gamma_1\le\theta\le\gamma_2. \tag{7}$$

Here $I_\nu(\rho)$, $K_\nu(\rho)$ are modified Bessel and Macdonald functions; $\rho=sr$, $\rho_0=sr_0$; $s=-ik$;

$$B_n=-\rho_0^{1/2}b_nI_\varphi^{(m)}\Psi_{\nu_n-1/2}(\cos\theta_0); \tag{8}$$

$\Psi_{\nu_n-1/2}(\cos\theta)$, $n=1,2,3,\ldots$ are the eigen-functions determined from the solution of Sturm-Liouville's problem as

$$\widehat{\Delta}_\theta\,\Psi_{\nu_n-1/2}=-(\nu_n^2-1/4)\Psi_{\nu_n-1/2},$$

which satisfies the boundary condition in Eq. (4) for $\theta = \gamma_1$ and $\theta = \gamma_2$, where

$$\widehat{\Delta}_\theta = \frac{1}{\sin\theta}\frac{\partial}{\partial\theta}\left(\sin\theta\frac{\partial}{\partial\theta}\right) - \frac{1}{\sin^2\theta}.$$

Functions $\Psi_{\nu_n-1/2}$ are bounded and orthogonal with weight $\sin\theta$ at the angle interval $\gamma_1 \le \theta \le \gamma_2$, and we represent these functions as

$$\Psi_{\nu_n-1/2}(\cos\theta) = \begin{cases} \dfrac{1}{\sin\theta},\ n=1, \\ \dfrac{\partial}{\partial\theta}[R_{\nu_n-1/2}(\cos\theta)],\ n>1, \end{cases} \tag{9}$$

where

$$R_{\nu-1/2}(\cos\theta) = P_{\nu-1/2}(\cos\theta)P_{\nu-1/2}(-\cos\gamma_1) - P_{\nu-1/2}(-\cos\theta)P_{\nu-1/2}(\cos\gamma_1), \tag{10}$$

$P_{\nu-1/2}(\cos\theta)$ is the Legendre function; $\{\nu_n\}_{n=1}^{\infty}$ is the growing sequence of real positive roots of transcendental equation

$$R_{\nu_n-1/2}(\cos\gamma_2) = 0 \tag{11}$$

with $\nu_1 = 1/2$ and $\nu_n \ne n - 1/2$ for $n = 2, 3, 4, \ldots$. The known coefficients b_n in Equation (8) are determined as

$$b_n = \begin{cases} \{\ln[ctg(\gamma_1/2)tg(\gamma_2/2)]\}^{-1},\ n=1, \\ 2\nu_n\left[\sin\gamma_2(\nu_n^2 - 1/4)\partial/\partial\nu R_{\nu_n-1/2}(\cos\gamma_2)\partial/\partial\gamma R_{\nu_n-1/2}(\cos\gamma_2)\right]^{-1},\ n>1. \end{cases}$$

The first term in the representation in Equation (7) corresponds to TEM-wave with two nonzero components in biconical area ($E_r \equiv 0, E_\theta, H_\varphi \ne 0$), and the other terms are elementary axially symmetric TM-modes. From expressions (2) and (7) it follows that the field components satisfy the radiation and boundary conditions, and for $r \to 0$ we arrive at

$$E_r = O(r^{\nu_2-3/2}), E_\theta = O(r^{-1}), H_\varphi = O(1). \tag{12}$$

Following from Equation (12), the TEM- and the lowest TM-modes determine the behaviour of E_θ-, H_φ- and E_r-components at the biconical vertex respectively. This shows that current density at the conical surfaces $J_r \sim rH_\varphi(r, \gamma_{1(2)}) \to 0$ for $r \to 0$ and the vertices of conical shoulders in Q (Q^∞) are electrically isolated.

3. SOLUTION OF THE DIFFRACTION PROBLEM

For the solution of the initial diffraction problem, let us introduce the regions as follows

$$D_1 : \{r \in (0, a_1), \theta \in [\gamma_1, \gamma_2)\},\ D_2 : \{r \in (0, a_1), \theta \in (\gamma_2, \pi]\},\ D_3 : \{r \in (a_1, \infty), \theta \in [\gamma_1, \pi]\}. \tag{13}$$

Since the unknown H_φ-field component satisfies Equation (3), we represent it by means of eigenfunctions in the appropriate domains as

$$H_\varphi(\rho,\theta) = \begin{cases} \dfrac{i\omega\varepsilon}{\sqrt{\rho}}\displaystyle\sum_{n=1}^{\infty} x_n^{(1)}\Psi_{\nu_n-1/2}(\cos\theta)\frac{I_{\nu_n}(\rho)}{I_{\nu_n}(\rho_1)},\ (r,\theta)\in D_1, \\ \dfrac{i\omega\varepsilon}{\sqrt{\rho}}\displaystyle\sum_{n=1}^{\infty} x_n^{(2)}\frac{\partial}{\partial\theta}P_{\mu_n-1/2}(-\cos\theta)\frac{I_{\mu_n}(\rho)}{I_{\mu_n}(\rho_1)},\ (r,\theta)\in D_2, \\ \dfrac{i\omega\varepsilon}{\sqrt{\rho}}\displaystyle\sum_{n=1}^{\infty} x_n^{(3)}\frac{\partial}{\partial\theta}P_{z_n-1/2}(-\cos\theta)\frac{K_{z_n}(\rho)}{K_{z_n}(\rho_1)},\ (r,\theta)\in D_3. \end{cases} \tag{14}$$

Here $x_n^{(1)}$, $x_n^{(2)}$, $x_n^{(3)}$ are unknown expansion coefficients; $\rho_1 = sa_1$; $\{z_n\}_{n=1}^{\infty}$, $\{\mu_n\}_{n=1}^{\infty}$ are growing sequences of the real positive roots of transcendental equations

$$P_{z_n-1/2}(-\cos\gamma_1) = 0, \tag{15a}$$

$$P_{\mu_n-1/2}(-\cos\gamma_2) = 0. \tag{15b}$$

The conditions in Equations (11), (15) guarantee satisfying the boundary condition in Equation (4) at the conical surfaces for field presentation in Equation (14), as well as the finiteness of energy in the vertex, and the radiation condition at infinity.

To find the unknown expansion coefficients in Equation (14), we use the mode matching as

$$H_{\varphi}^{D_3}|_{r=a_1+0}_{\gamma_1<\theta<\pi} = \begin{pmatrix} H_{\varphi}^{D_2}|_{r=a_1-0}, \\ {\scriptstyle \gamma_2<\theta<\pi} \\ H_{\varphi}^{D_1}|_{r=a_1-0} + H_{\varphi}^{(i)}|_{r=a_1-0}; \\ {\scriptstyle \gamma_1<\theta<\gamma_2} \end{pmatrix} \quad E_{\theta}^{D_3}|_{r=a_1+0}_{\gamma_1<\theta<\pi} = \begin{pmatrix} E_{\theta}^{D_2}|_{r=a_1-0}, \\ {\scriptstyle \gamma_2<\theta<\pi} \\ E_{\theta}^{D_1}|_{r=a_1-0} + E_{\theta}^{(i)}|_{r=a_1-0}. \\ {\scriptstyle \gamma_1<\theta<\gamma_2} \end{pmatrix} \tag{16}$$

Here $H_{\varphi}^{D_\alpha}(\rho,\theta)$, $E_{\theta}^{D_\alpha}(\rho,\theta)$, $\alpha = 1,2,3$ are diffracted field in D_1 and total field in D_2, D_3. In order to take into account the singularity of $E_{\theta}^{t}(r,\theta) = O(\widehat{\rho}^{-1/2})$ for $\widehat{\rho}\to 0$, where $\widehat{\rho}$ is the distance to the edge in local coordinate system. We present these equations by way of

$$\lim_{N\to\infty}\sum_{\substack{n=1\\(r,\theta)\in D_3}}^{N} x_n^{(3)} P^1_{z_n-1/2}(-\cos\theta) = \begin{cases} -\lim\limits_{K\to\infty}\sum\limits_{k=1}^{K}\left[x_k^{(1)} + B_k K_{\nu_k}(\rho_1) I_{\nu_k}(\rho_0)\right]\Psi_{\nu_k-1/2}(\cos\theta), \\ \qquad\qquad (r,\theta)\in D_1 \\ \lim\limits_{P\to\infty}\sum\limits_{p=1}^{P} x_p^{(2)} P^1_{\mu_p-1/2}(-\cos\theta); \\ \qquad\qquad (r,\theta)\in D_2 \end{cases} \tag{17a}$$

$$\lim_{N\to\infty}\sum_{\substack{n=1\\(r,\theta)\in D_3}}^{N} x_n^{(3)} P^1_{z_n-1/2}(-\cos\theta)\frac{K'_{z_n}(\rho_1)}{K_{z_n}(\rho_1)} = \begin{cases} -\lim\limits_{K\to\infty}\sum\limits_{k=1}^{K}\left[x_k^{(1)}\dfrac{I'_{\nu_n}(\rho_1)}{I_{\nu_n}(\rho_1)} + B_k K'_{\nu_k}(\rho_1) I_{\nu_k}(\rho_0)\right]\Psi_{\nu_k-1/2}(\cos\theta), \\ \qquad\qquad (r,\theta)\in D_1 \\ \lim\limits_{P\to\infty}\sum\limits_{p=1}^{P} x_p^{(2)} P^1_{\mu_p-1/2}(-\cos\theta)\dfrac{I'_{\mu_n}(\rho_1)}{I_{\mu_n}(\rho_1)}. \\ \qquad\qquad (r,\theta)\in D_2 \end{cases} \tag{17b}$$

Here known coefficients B_k, $k = 1,2,3,\ldots$ are defined in Equation (8); $P^1_{\eta-1/2}(\cdot)$ is the associated Legendre function, which is defined in [36] by the expression $P^1_{\nu-1/2}(\pm\cos\theta) = \pm\partial/\partial\theta[P_{\nu-1/2}(\pm\cos\theta)]$; the prime indicates the derivation with respect to the argument.

In order to reduce series Equations (17) to ISLAE, we use a property of orthogonality of Legendre functions, which leads to [32]

$$P^1_{z_n-1/2}(-\cos\theta) = q(z_n,\gamma_2)\begin{cases} -\lim\limits_{K\to\infty}\sum\limits_{k=1}^{K}\dfrac{\alpha(\nu_k;\gamma_1,\gamma_2)}{\nu_k^2 - z_n^2}\Psi_{\nu_k-1/2}(\cos\theta), \ \text{for } \gamma_1\le\theta<\gamma_2, \\ \lim\limits_{P\to\infty}\sum\limits_{p=1}^{P}\dfrac{\alpha(\mu_p;\gamma_2)}{\mu_p^2 - z_n^2}P^1_{\mu_p-1/2}(-\cos\theta), \ \text{for } \gamma_2<\theta\le\pi. \end{cases} \tag{18}$$

Here

$$\begin{aligned} q(z_n,\gamma_2) &= (z_n^2 - 1/4)P_{z_n-1/2}(-\cos\gamma_2), \\ \alpha(\nu_k;\gamma_1,\gamma_2) &= -\begin{cases} \{\ln[\mathrm{ctg}(\gamma_1/2)\mathrm{tg}(\gamma_2/2)]\}^{-1}, \ k=1, \\ 2\nu_k\left[(\nu_k^2-1/4)\partial/\partial\nu R_{\nu_k-1/2}(\cos\gamma_2)\right]^{-1}, \ k>1, \end{cases} \\ \alpha(\mu_p;\gamma_2) &= -2\mu_p\left[(\mu_p^2-1/4)\partial/\partial\mu P_{\mu_p-1/2}(-\cos\gamma_2)\right]^{-1}. \end{aligned}$$

Then we prove the following theorem on the convergence of the series in Equation (18):
Theorem. For all γ_2 which belongs to $\gamma_1 < \gamma_2 < \pi$, the upper and lower series on the right-hand part of Equation (18) are uniformly convergent to the function $P^1_{z_n-1/2}(-\cos\theta)/q(z_n,\gamma_2)$ for any $\theta \in [\gamma_1,\gamma_2]$ and $\theta \in [\gamma_2,\pi]$ respectively.
Proof. Let us consider the integral as follows

$$J_n(\theta) = \frac{1}{2\pi i}\int\limits_{C_R} \frac{t\Psi_{t-1/2}(\cos\theta)dt}{(t^2-z_n^2)(t^2-1/4)R_{t-1/2}(\cos\gamma_2)}. \tag{19}$$

Here $\Psi_{t-1/2}(\cos\theta) = \partial/\partial\theta\,[R_{t-1/2}(\cos\theta)]$; C_R is the circular integration path in complex plane t, the point $t = 0$ and R are the center and radius of this circle respectively; C_R outline encompasses the simple poles of the integrand at $t = \pm 1/2$, $t = \pm z_n$ and $t = \pm\nu_k$ $(k = 1, 2, 3, \ldots)$. For $|t| \to \infty$ the integrand as a function of t tends to zero not slower than t^{-2}, therefore $J_n(\theta) \to 0$ if $R \to \infty$. Then, taking into account that

$$\lim_{t\to\pm 1/2} \frac{\partial/\partial\theta\,[R_{t-1/2}(\cos\theta)]}{R_{t-1/2}(\cos\theta)} = \frac{1}{\ln[\mathrm{ctg}(\gamma_1/2)\mathrm{tg}(\gamma_2/2)]\sin\theta} \tag{20}$$

and applying the residues theorem, we arrive at the statement of the theorem for $\theta \in [\gamma_1,\gamma_2]$. For $\theta \in [\gamma_2,\pi]$ the theorem can be proved in the same way.

Let us substitute the series in Equation (18) into Equations (17). Next, limiting the finite number of unknowns and excluding $x_k^{(1)}$, $x_p^{(2)}$, we come to the finite system of linear algebraic equations as follows

$$\begin{aligned} &\sum_{n=1}^{N} \frac{x_n}{\mu_p^2 - z_n^2} \frac{\rho_1 W[K_{z_n} I_{\mu_p}]_{\rho_1}}{I_{\mu_p}(\rho_1)K_{z_n}(\rho_1)} = 0,\ p = \overline{1,P}, \\ &\sum_{n=1}^{N} \frac{x_n}{\nu_k^2 - z_n^2} \frac{\rho_1 W[K_{z_n} I_{\nu_k}]_{\rho_1}}{I_{\nu_k}(\rho_1)K_{z_n}(\rho_1)} = \bar{f}_k,\ \ k = \overline{1,K}, \end{aligned} \tag{21}$$

where $x_n = q(z_n,\gamma_2)x_n^{(3)}$, $W[f,\phi]_\rho = f(\rho)\phi'(\rho) - f'(\rho)\phi(\rho)$, $N = P + K$;

$$\bar{f}_k = \sqrt{\rho_0} I_\varphi^{(m)} d_k \Psi_{\nu_k-1/2}(\cos\theta_0)\frac{I_{\nu_k}(\rho_0)}{I_{\nu_k}(\rho_1)}, \quad |\rho_0| < |\rho_1|, \tag{22}$$

$$d_k = \begin{cases} 1,\ k = 1, \\ [\sin\gamma_2 \partial/\partial\gamma R_{\nu_k-1/2}(\cos\gamma_2)]^{-1},\ k > 1. \end{cases}$$

The reason we introduce this limitation is to provide the correct transition from Equations (17) to the ISLAE $(P,K,N \to \infty)$, the solution of which satisfies the Meixner condition at the conical edge. For this purpose, we introduce a growing sequence of roots $\{\nu_k\}_{k=1}^\infty$, $\{\mu_p\}_{p=1}^\infty$ of transcendental Equations (11), (15b) as

$$\{\xi_j\}_{j=1}^\infty = \{\nu_k\}_{k=1}^\infty \cup \{\mu_p\}_{p=1}^\infty. \tag{23}$$

Next, in Equations (21) we pass to the limit $P,K,N \to \infty$ $(N = P + K)$ and arrange the ISLAE according to sequence (23) as

$$A_{11}X = F. \tag{24}$$

Here $X = \{x_n\}_{n=1}^\infty$ is the unknown vector, $x_n = x_n^{(3)}(z_n^2 - 0.25)P_{z_n-1/2}(-\cos\gamma_2)$; A_{11} is the infinite matrix with the elements given as

$$A_{11} : \left\{ a_{jn}^{(11)} = \frac{\rho_1 W[K_{z_n} I_{\xi_j}]_{\rho_1}}{[\xi_j^2 - z_n^2] I_{\xi_j}(\rho_1)K_{z_n}(\rho_1)} \right\}_{j,n=1}^{\infty}; \tag{25}$$

$F = \{f_j\}_{j=1}^\infty$ is the known vector with

$$f_j = \begin{cases} \bar{f}_j, & \xi_j \in \{\nu_k\}_{k=1}^\infty, \\ 0, & \xi_j \notin \{\nu_k\}_{k=1}^\infty. \end{cases} \tag{26}$$

The well-known particular case of the excitation of the bi-cone Q by TEM-mode, we obtain from Equation (7) having turn $\rho_0 \to 0$ as

$$H^i_\varphi(r,\theta) = -\frac{i\omega\varepsilon C}{\ln[\mathrm{ctg}(\gamma_1/2)\mathrm{tg}(\gamma_2/2)]}\frac{K_{1/2}(\rho)}{\sin\theta\sqrt{\rho}}\,,\ |\rho| > 0$$

with $C = \lim\limits_{\rho_0\to 0}\{I^{(m)}_\varphi(\rho_0,\theta_0)\sqrt{\rho_0}I_{1/2}(\rho_0)/\sin\theta_0\} = \text{const}$. This leads to the simplification of Equation (22) as $\bar{f}_j = C\{I_{1/2}(\rho_1)\}^{-1}$ for $j=1$ and $\bar{f}_j = 0$ for $j>1$.

Next, we apply the analytical regularization procedure for reducing ISLAE in Equation (24) to the ISLAE of the second kind.

4. REGULARIZATION OF ISLAE

Taking into account the asymptotic properties of the modified Bessel and Macdonald functions for large indices [36], we find that

$$a^{(11)}_{jn} = \frac{1}{\xi_j - z_n} + \begin{cases} O\left(\langle \xi_j z_n(\xi_j - z_n)\rangle^{-1}\right), & \xi_j, z_n >> |sa_1|; \\ O\left((sa_1/2)^2\right), & |sa_1| \to 0. \end{cases} \tag{27}$$

Let us introduce the operator formed with the main parts of the asymptotic expression (27) and the inverse operator as [32, 35]

$$A : \left\{a_{jn} = \langle \xi_j - z_n\rangle^{-1}\right\}^\infty_{j,n=1}, \tag{28a}$$

$$A^{-1} : \left\{\tau_{kj} = \left\langle \{M^{-1}_-(\xi_j)\}' M'_-(z_k)(z_k - \xi_j)\right\rangle^{-1}\right\}^\infty_{k,j=1}. \tag{28b}$$

Here, the product of operators in Equation (28) represents the identity matrix I, $A^{-1}A = I$ [32, 33];

$$\{[M_-(\xi_j)]^{-1}\}' = \frac{\partial}{\partial\nu}\left[M_-(\xi_j)\right]^{-1}, \quad M'_-(z_n) = \frac{\partial}{\partial\nu}\left[M_-(z_n)\right],$$

where $M_-(\nu)$ is determined from the factorization of the even meromorphic function $M(\nu)$, which is regular in the strip $\Pi : \{|\mathrm{Re}\nu| < 1/2\}$ with simple zeroes and poles at $\nu = \pm z_k$, $\nu = \pm\xi_j$ that are located at the real axis out of the Π;

$$M(\nu) = M_+(\nu)M_-(\nu) = \frac{P_{\nu-1/2}(-\cos\gamma_1)\cos(\pi\nu)}{(\nu^2 - 1/4)P_{\nu-1/2}(-\cos\gamma_2)R_{\nu-1/2}(\cos\gamma_2)}, \tag{29}$$

$M_+(\nu)$, $M_-(\nu)$ are split functions, regular in the right $\mathrm{Re}\nu > -1/2$ and in the left $\mathrm{Re}\nu < 1/2$ half-planes respectively; $M(\nu) = O(\nu^{-1})$ and $M_+(\nu) = M_-(-\nu) = O(\nu^{-1/2})$ if $|\nu| \to \infty$ in the regularity region;

$$M_-(\nu) = \frac{2A(\gamma_1,\gamma_2)e^{\nu\chi}\prod\limits_{k=1}^\infty (1-\nu/z_k)e^{\nu(\pi-\gamma_1)/(k\pi)}}{(1-\nu/(1/2))\prod\limits_{k=1}^\infty (1-\nu/\mu_k)e^{\nu(\pi-\gamma_2)/(k\pi)}\prod\limits_{k=1}^\infty (1-\nu/\nu_{k+1})e^{\nu(\gamma_2-\gamma_1)/(k\pi)}},$$

where

$$A(\gamma_1,\gamma_2) = \mathrm{i}\left[\frac{P_{-1/2}(-\cos\gamma_1)}{P_{-1/2}(-\cos\gamma_2)\left[P_{-1/2}(\cos\gamma_2)P_{-1/2}(-\cos\gamma_1) - P_{-1/2}(-\cos\gamma_2)P_{-1/2}(\cos\gamma_1)\right]}\right]^{1/2},$$

$$\chi = \frac{\pi-\gamma_2}{\pi}\ln\frac{\pi-\gamma_2}{\pi} - \frac{\pi-\gamma_1}{\pi}\ln\frac{\pi-\gamma_1}{\pi} + \frac{\gamma_2-\gamma_1}{\pi}\ln\frac{\gamma_2-\gamma_1}{\pi}.$$

The formulas for effective calculation the matrix elements τ_{kj} in Equation (28b) are presented in **Appendix A**.

Next, we formulate original diffraction problem via the ISLAE of the second kind as follows

$$X - A^{-1}(A - A_{11})X = A^{-1}F. \tag{30}$$

The technique described above is elaborated in [32–34] and called the analytical regularization procedure. ISLAE in Equation (30) admits the solution in the class of sequences $b(\sigma) : \{||X|| = \sup_n |x_n|,\ \lim_{n\to\infty} |x_n n^\sigma| \to 0\}$ for $0 \le \sigma < 1/2$. This fulfills all the necessary conditions for the existence of a unique solution of ISLAE in Equation (30), including the Meixner condition on the edge.

The proof of these statements is based on the use of asymptotic estimates for matrix elements in Equations (25) and (28b), that are given in the expression (27) and by the formula

$$\tau_{nj} \underset{j,n\to\infty}{=} O\left(\frac{\xi_j^{-1/2} z_n^{1/2}}{z_n - \xi_j}\right). \tag{31}$$

ISLAE (30) is valid for $\gamma_{1(2)} \neq \pi/2$ ($\gamma_2 > \gamma_1$).

We represent unknown coefficients in (14) through the solution (30) by way of

$$\begin{aligned} x_j^{(1)} &= -\alpha(\nu_j;\gamma_1,\gamma_2)K_{\nu_j}(\rho_1)I_{\nu_j}(\rho_1)\sum_{n=1}^{\infty}\frac{x_n}{\nu_j^2 - z_n^2}\frac{\rho_1 W[K_{\nu_j}K_{z_n}]_{\rho_1}}{K_{\nu_j}(\rho_1)K_{z_n}(\rho_1)}, \\ x_j^{(2)} &= \alpha(\mu_j;\gamma_2)K_{\mu_j}(\rho_1)I_{\mu_j}(\rho_1)\sum_{n=1}^{\infty}\frac{x_n}{\mu_j^2 - z_n^2}\frac{\rho_1 W[K_{\mu_j}K_{z_n}]_{\rho_1}}{K_{\mu_j}(\rho_1)K_{z_n}(\rho_1)}, \\ x_j^{(3)} &= x_j/q(z_j,\gamma_2). \end{aligned} \tag{32}$$

Taking into account the correlations in Equations (2), (14) and (32), we get the definitive expressions for field representation anywhere in biconical and conical regions.

5. LOW FREQUENCY SOLUTION

Let us rewrite the basic ISLAE in Equation (30) by way of

$$x_k = \sum_{q=1}^{\infty}\tau_{kq}\sum_{n=1}^{\infty}(a_{qn} - a_{qn}^{(11)})x_n + \sum_{q=1}^{\infty}\tau_{kq}f_q, \tag{33}$$

where $k = 1, 2, 3, \ldots$.

We take into account the low frequency ($|sa_1| \to 0$) asymptotic expression (27) and estimate the terms in Equations (25) and (32) as

$$I_{\nu_k}(sr_0)/I_{\nu_k}(sa_1) = (r_0/a_1)^{\nu_k}\left[1 + O((sr_0/2)^2, (sa_1/2)^2)\right] \tag{34}$$

$$sa_1 W[K_{\eta_j}K_{z_n}]_{sa_1}/[(\eta_j^2 - z_n^2)K_{\eta_j}(sa_1)K_{z_n}(sa_1)] = 1/(\eta_j + z_n) + O((sa_1/2)^2), \tag{35}$$

where

$$\eta_j = \nu_j(\mu_j).$$

Neglecting the terms of order $|sa_1/2|^2$ and $|sr_0/2|^2$, we immediately derive the approximate solution (32) as

$$x_k = \sqrt{sr_0}I_\varphi^{(m)}\left[\frac{\tau_{k1}}{\sin\theta_0}\left(\frac{r_0}{a_1}\right)^{1/2} + \sum_{q=2}^{\infty}\tau_{kq}d_q\Psi_{\nu_q-1/2}(\cos\theta_0)\left(\frac{r_0}{a_1}\right)^{\nu_q}\right], \tag{36}$$

and

$$\begin{aligned} x_j^{(1)} &= -\frac{\alpha(\nu_j;\gamma_1,\gamma_2)}{2\nu_j}\sum_{q=1}^{\infty}c_q(\nu_j)f_q, \\ x_j^{(2)} &= \frac{\alpha(\mu_j;\gamma_2)}{2\mu_j}\sum_{q=1}^{\infty}c_q(\mu_j)f_q, \end{aligned} \tag{37}$$

where

$$c_q(\eta_j) = \sum_{n=1}^{\infty} \frac{\tau_{nq}}{\eta_j + z_n}. \tag{38}$$

Let us introduce a contour integral

$$J_{jq} = \frac{1}{2\pi i} \int\limits_{C_R} \frac{1}{(\eta_j + t)(t - \xi_q) M_-(t)} dt, \tag{39}$$

where the circle C_R with radius $|t| = R$ that envelopes the simple poles of the integrand at $t = z_n$ $(n = 1, 2, 3 \ldots)$ and $t = -\eta_j$. The integrand in Equation (39) decays as $t^{-3/2}$, if $R \to \infty$. Next, using the residual theorem and Equation (28b), it is found that

$$c_q(\eta_j) = \frac{1}{[M_-^{-1}(\xi_q)]' M_+(\eta_j)(\eta_j + \xi_q)}. \tag{40}$$

Equations (36), (37) and (40) give the approximate solution of the diffraction problem in low-frequency case.

6. TRANSITION TO THE CONICAL MONOPOLE ($\gamma_1 = \pi/2$) AND TO THE DISC-CONE SCATTERER ($\gamma_2 = \pi/2$)

For these two particular cases the wave diffraction problems are reduced to ISLAE in Equation (30) by the same way as in the general case. Here instead of using Equation (11), we use the transcendental equation

$$P_{\nu_n - 1/2}(\cos\gamma_\alpha) - P_{\nu_n - 1/2}(-\cos\gamma_\alpha) = 0, \tag{41}$$

where $\alpha = 1, 2$ for disc-cone and conical monopole respectively, to determine the indexes $\nu_n > 0$ $(n = 1, 2, 3, \ldots)$ for eigen function for the bi-conical region ($\nu \neq 2n + 1/2$, $\nu_1 = 1/2$). Taken this into account, we derive the regularization operator in Equation (28b) using the functions

$$M(\nu) = \begin{cases} \dfrac{\cos(\pi\nu)}{(\nu^2 - 1/4) P_{\nu-1/2}(-\cos\gamma_2) \left[P_{\nu-1/2}(\cos\gamma_2) - P_{\nu-1/2}(-\cos\gamma_2)\right]}, \\ \qquad \text{for monopole } (\gamma_1 = \pi/2), \\ \dfrac{P_{\nu-1/2}(-\cos\gamma_1)\cos(\pi\nu)}{(\nu^2 - 1/4)\left[P_{\nu-1/2}(0)\right]^2 \left[P_{\nu-1/2}(-\cos\gamma_1) - P_{\nu-1/2}(\cos\gamma_1)\right]}, \\ \qquad \text{for disc-cone } (\gamma_2 = \pi/2). \end{cases} \tag{42}$$

that are obtained from kernel function in Equation (29), if $\gamma_{1(2)} \to \pi/2$. The eigen-functions for bi-conical region $\Psi_{\nu_n - 1/2}(\cos\theta)$ are determined here as in Equation (9) with

$$R_{\nu_n - 1/2}(\cos\theta) = P_{\nu_n - 1/2}(-\cos\theta) - P_{\nu_n - 1/2}(\cos\theta). \tag{43}$$

7. NUMERICAL CALCULATION

All characteristics of the scattered field are calculated by reduction of ISLAE in Equation (30). The order of reduction has been chosen from the condition $N = |sa_1| + q$ with $q = (4 \div 10)$. Based on the solution of finite system of linear algebraic equations, we analyze far-field characteristics for bi-cone Q with the different geometrical parameters and exiting source location.

Let us express the far-field pattern and radiation power as

$$D(\theta) = \lim_{r \to \infty} \left| r H_\varphi e^{-ikr} \right|, \tag{44}$$

$$W = \lim_{r \to \infty} \frac{1}{2} \int_0^{2\pi} d\phi \int_{\gamma_1}^{\pi} E_\theta H_\phi^* r^2 \sin\theta d\theta, \tag{45}$$

where H_φ and E_θ for their physical matter determine the total field components in region D_3; upper mark (*) shows the complex conjugate.

We have calculated the dimensionless components as $[Z/(kI_\varphi^{(m)})]H_\varphi$ and $[1/(kI_\varphi^{(m)})]E_\theta$. The curves presented here show the characteristics of the field, diffracted from the bi-cone, which is excited by the magnetic current of the unit amplitude. Such electrodynamic system is placed in a hypothetical environment with single electrical and single magnetic parameters. With the help of Equations (44), (45), we analyze the scattering properties of the bi-cone Q. We focus here on the two important cases and consider the diffraction from the conical monopoles and disco-conical scatterers, which we obtain from Q with $\gamma_1 \to \pi/2$, $\pi/2 < \gamma_2 < \pi$ and $\gamma_2 \to \pi/2$, $0 < \gamma_1 < \pi/2$ respectively.

In most papers the considered monopoles are excited by sources located near the conical vertex. This ensures the best symmetry of the field and the domination of the lower TEM-mode in the excited source. To determine the influence of the higher excitatory modes on the far field formation let us analyze the influence of the source location on such formation. Here we model the conical monopoles using the bi-cones with $\gamma_1 = 89°$. Due to the symmetry of the far field distribution we plot the radiation patterns only for $90° < \theta < 180°$ (see Fig. 2).

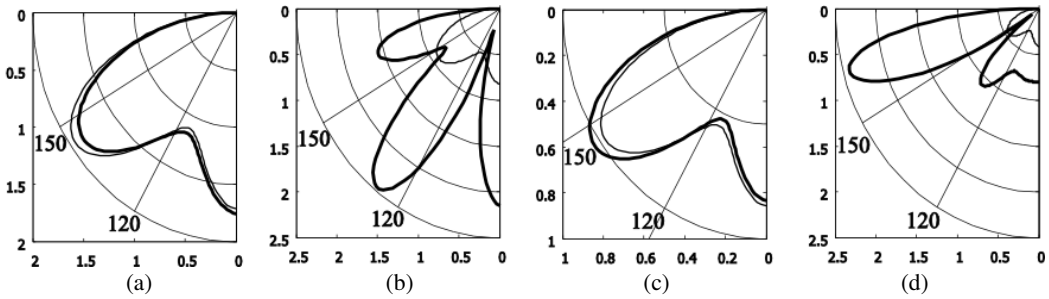

Figure 2. Influence of the source location on the far field patterns of conical monopoles for $\gamma_1 = 89°$, $\gamma_2 = 150°$; $ka_1 = 6.28$; (a), (c) $kr_0 = 1.0$; (b), (d) $kr_0 = 5.87$; (a), (b) $\theta_0 = \gamma_2$; (c), (d) $\theta_0 = \gamma_1$. The thin lines represent the excitation by TEM-mode. The thick lines represent the excitation by all modes of the source.

The bold curves in this figure correspond to the case, when all the necessary modes radiated by the source are taken into account, including TEM-mode. The thin line shows the far field distribution, which takes into consideration only the lowest TEM-mode.

Let us consider two cases. In the first case, the ring magnetic current is located on the finite shoulder (Fig. 2(a), 2(b)), and in the second case, it is located on the plane (Figs. 2(c), 2(d)). As follows from Figs. 2(a), 2(c), the radiation field in these two cases is formed by TEM-source's wave, if $kr_0 \leq 1.0$.

When the source moves away from the top of the cone and $r_0 > \lambda/2$, where λ is the wavelength, the excitation of the higher source's modes becomes effective, and the far field patterns change significantly (Figs. 2(b), 2(d)). As follows from this figure, the radius of the source affects the shape of the far field patterns significantly, regardless of the shoulder on which the source is located.

To estimate the potential possibilities of control of the radiation patterns, we investigate the influences of the opening angle γ_2 on the far field distribution. These influences for the two lengths of the shoulder are shown in Fig. 3. To simplify the analysis we place the source near the top of the cone. As follows from Fig. 3, the frequent oscillations of the far field are observed in the shady region $\gamma_2 < \theta < \pi$. The frequency of these oscillations increase with the increase of the length of the shoulder, and for $\gamma_2 < 130°$ the major radiation is directed along the plane. The growth of the parameter γ_2 leads to narrowing of the conical cavity and to turning of the main lobe of the far field in the direction of the monopole's generatrix.

Next, we plot the monopole's radiation power as functions of the shoulder length for several opening angles γ_2 to analyze its wide-band scattering characteristics (see Fig. 4(a)). In this figure we observe the effect of the resonance power scattering, if $ka_1 = 2.0 \div 2.2$. We observe this phenomenon for different

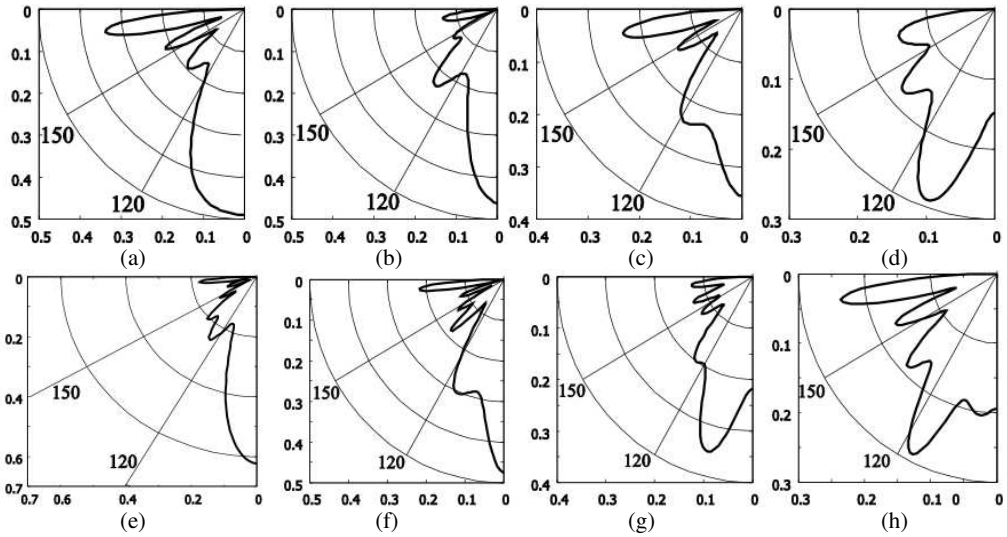

Figure 3. Influence of the opening angle γ_2 on the far field magnitude of the monopole for $\gamma_1 = 89°$; $kr_0 = 0.2$; $\theta_0 = \gamma_1$; (a), (e) $\gamma_2 = 110°$; (b), (f) $\gamma_2 = 120°$; (c), (g) $\gamma_2 = 130°$; (d), (h) $\gamma_2 = 140°$; (a)–(d) $ka_1 = 12.56$; (e)–(h) $ka_1 = 18.84$.

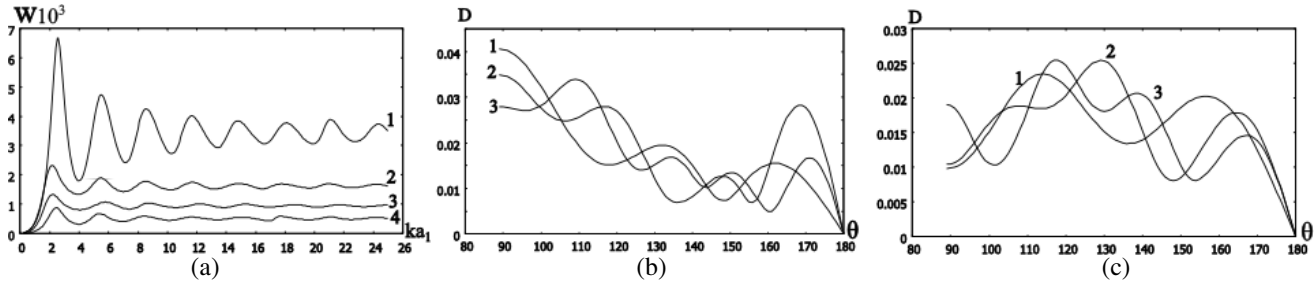

Figure 4. Dependencies of the conical monopole radiation power on the ka_1 (a) for $kr_0 = 0.02$; $\gamma_1 = 89°$, $\theta_0 = \gamma_1$; 1 $\gamma_2 = 110°$; 2 $\gamma_2 = 130°$; 3 $\gamma_2 = 150°$; 4 $\gamma_2 = 170°$. Far field patterns of the monopole (b), (c) for: 1 $ka_1 = 9$; 2 $ka_1 = 12$; 3 $ka_1 = 15$; (b) $\gamma_2 = 130°$; (c) $\gamma_2 = 150°$.

angles γ_2. The maximum of monopole's radiation power can be seen for scatterers with the narrow bi-conical area (curve 1 in Fig. 4(a), $\Delta\gamma_{21} = 21°$, $\Delta\gamma_{21} = \gamma_2 - \gamma_1$).

The growth of the bi-conical region leads to falling of the resonance maximum. As follows from Fig. 4(a), the growth of the bi-conical area from $\Delta\gamma_{21} = 21°$ (curve 1) to $\Delta\gamma_{21} = 81°$ (curve 4) reduces the resonance peak almost by one order of magnitude. From this figure we also see that the radiation power from monopoles with a wide bi-conical area ($\Delta\gamma_{21} > 40°$) and $ka_1 > 5$ practically does not depend on ka_1. Therefore, it is possible that monopoles with such parameters possess the wide-band scattering properties. Figs. 4(b), 4(c) show the influence of the shoulder length on the far field pattern of the monopole with different width of bi-conical area. As follows from these figures, the increase of the monopole's shoulder length from $ka_1 = 9$ to $ka_1 = 15$ does not significantly influence the far field patterns all over the angular range of radiation for the monopoles with wide bi-conical area ($\Delta\gamma_{21} > 40°$). This confirms the wide-band properties of conical monopoles.

Let us consider the disc-conical antenna formed by the bi-cone Q with $\gamma_2 = 89°$ and $\gamma_1 < \gamma_2$ to analyze its scattering characteristics and compare them with the conical monopole scattering properties. The influences of the source location on the far field patterns for disc-conical scatter are shown in the Fig. 5. The far field diffracted from disc-cone is also totally formed by the lowest TEM-source's wave if $kr_0 \leq 1.0$ (see Figs. 5(a), 5(c)). The higher source's modes become effective and the far field patterns

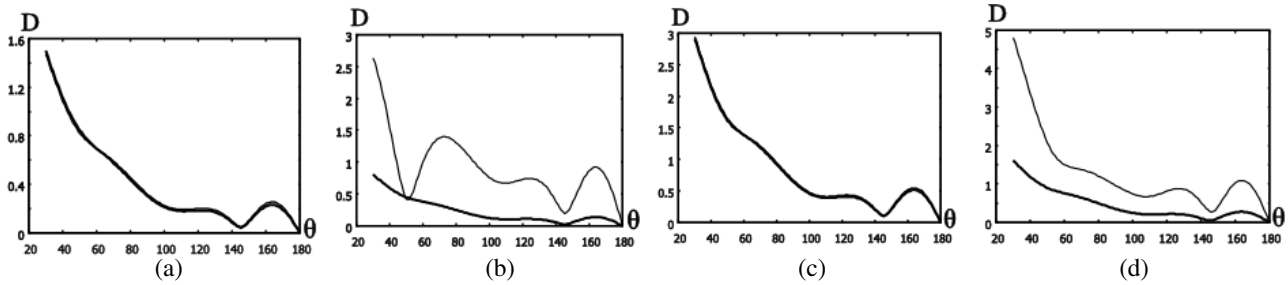

Figure 5. Influences of the source location on the far field patterns of disc-cone for $\gamma_1 = 30°$, $\gamma_2 = 89°$, $ka_1 = 6.28$; (a), (c) $kr_0 = 1.0$; (b), (d) $kr_0 = 3.62$; (a), (b) $\theta_0 = \gamma_2$; (c), (d) $\theta_0 = \gamma_1$. The thin lines represent the excitation by TEM-mode. The thick lines represent the excitation by all modes of the source.

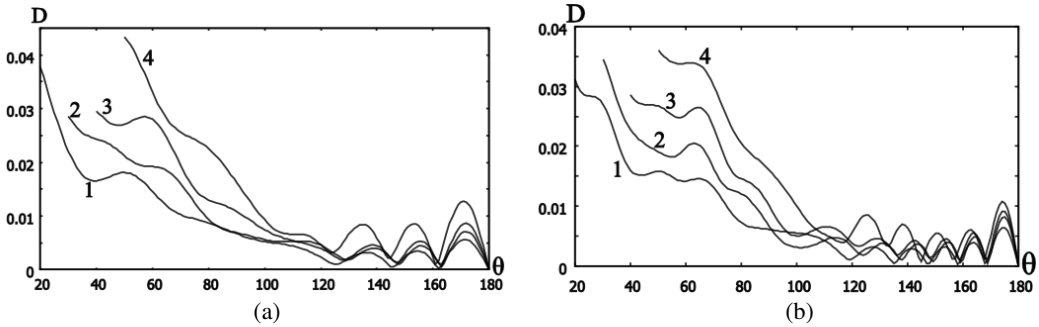

Figure 6. Influences of the opening angle γ_1 on the far field diffracted from disc-cone for $\gamma_2 = 89°$, $\theta_0 = \gamma_2$, $kr_0 = 0.02$; 1 $\gamma_1 = 20°$; 2 $\gamma_1 = 30°$; 3 $\gamma_1 = 40°$; 4 $\gamma_1 = 50°$; (a) $ka_1 = 12.56$; (b) $ka_1 = 18.84$.

change significantly, if $r_0 > \lambda/2$ (see Figs. 5(b), 5(d)).

Next, we investigate the influence of the conical angle γ_1 on the far field scattered by the disc-cone. These influences for the different radiuses of the disc are shown in Fig. 6. As follows from Fig. 6, the main radiation of the disc-cone is directed along the semi-infinite conical surface for all the considered angles γ_1. In this figure we also observe the far field patterns in the shadow region (see Fig. 6, $\pi/2 < \theta < \pi$) and find that they are similar to those well-known for the disc illuminated axial-symmetrically in free space [32].

Here we see the field oscillations that do not depend on the width of the bi-conical region $\Delta\gamma_{21}$. Their frequency is growing with the growth of the disc's radius, and the main maximum in the shadow region is located close to the axis of symmetry of the disc-cone. The far field distribution for the disc-cone in the lighted region ($\gamma_1 < \theta < \pi/2$) depends significantly on angle γ_1 (see Figs. 6(a), 6(b)).

To study the wide-band scattered characteristics of the disc-cone we analyze its radiation power a functions of the disc's radius for different values γ_1 (see Fig. 7(a)). In this figure we observe the effect of resonance scattering, if $ka_1 = 2.0 \div 3.0$ for different angles γ_1. The maximum of resonance radiation is observed for the disc-cone with the narrow bi-conical region (see curve 4 in Fig 7(a), $\Delta\gamma_{21} = 21°$). Here we also see that the extension of the bi-conical region of the disc-cone's scatterer leads to the fall of the resonance maximum. As follows from Fig. 7(a), the extension of the bi-conical area from $\Delta\gamma_{21} = 21°$ (see curve 4) to $\Delta\gamma_{21} = 81°$ (see curve 1) reduces the resonance peak by more than one order of magnitude.

In this figure we also see that the radiation power from the disc-cone with wide bi-conical area ($\Delta\gamma_{21} > 50°$) and $ka_1 > 9$ practically does not depend on ka_1. Therefore, it is possible that the disc-cones with such parameters possess the wide-band scattering properties. Figs. 7(b), 7(c) show the influence of the length of the disc's radius on the far field scattered by the disc-cone with different width of bi-conical area.

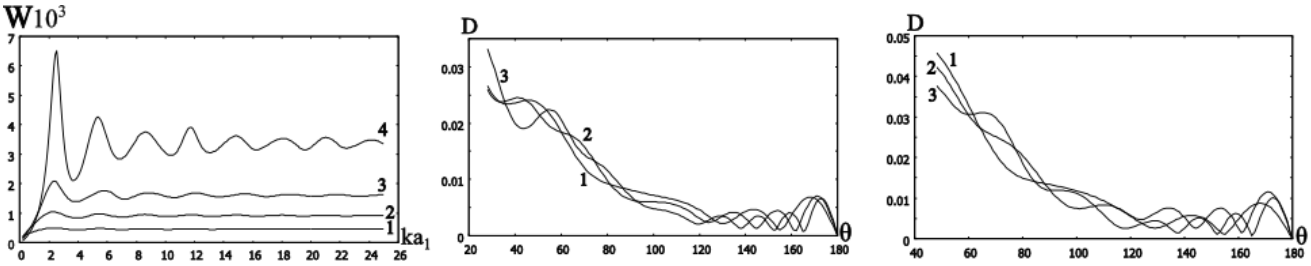

(a) (b) (c)

Figure 7. Dependencies of the disc-cone radiation power on the ka_1 (a) for $\gamma_2 = 89°$, $\theta_0 = \gamma_2$; $kr_0 = 0,02$; 1 $\gamma_1 = 8°$; 2 $\gamma_1 = 28°$; 3 $\gamma_1 = 48°$; 4 $\gamma_1 = 68°$. Far field patterns of the disc-cone (b), (c) for 1 $ka_1 = 9$; 2 $ka_1 = 12$; 3 $ka_1 = 15$; (b) $\gamma_1 = 28°$; (c) $\gamma_1 = 48°$.

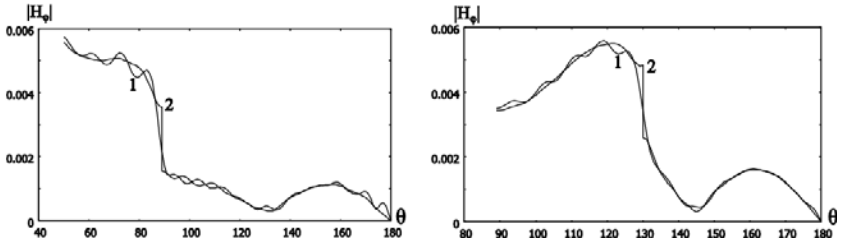

(a) (b)

Figure 8. Testing the satisfaction of the mode-matching condition on the spherical segment with $r = a_1$, $ka_1 = 6.28$, $kr_0 = 0,02$: (a) $\gamma_1 = 50°$,$\gamma_2 = 89°$, $\theta_0 = \gamma_2$; (b) $\gamma_1 = 89°$, $\gamma_2 = 130°$, $\theta_0 = \gamma_1$, 1 $r = a_1 + 0$; 2 $r = a_1 - 0$.

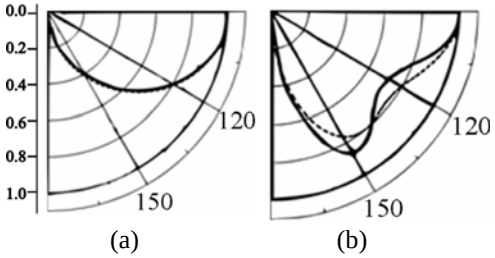

(a) (b)

Figure 9. Comparison of the normalized far field patterns for hollow and closed conical monopoles with $\gamma_1 = 89°$, $\gamma_2 = 150°$, $\theta_0 = \gamma_2$; $kr_0 = 0.2$; (a) $ka_1 = 1.0$; (b) $ka_1 = 5.0$.

The behavior of the curves in these figures shows the wide-band properties of the disc-cone that look better than those for the conical monopole because here we observe the lesser influence of the frequency parameter on the distribution of the far field.

To verify the calculations we test the satisfaction of the mode-matching conditions on the virtual spherical segment with radius $r = a_1$ for different bi-cones. Some typical results are presented in Fig. 8. Here we observe good adjustment $|H_\varphi|$ for all segment's area $\gamma_1 < \theta < \pi$.

We verify our results by comparing them to those obtained for conical monopole closed by the spherical segment and excited by TEM-wave. Fig. 9 shows the normalized far field magnitudes: the dashed line corresponds to the hollow monopole (our results), and the solid line corresponds to the closed monopole (obtained in [18]). In these figures we see a good agreement of the normalized field's magnitude for all observation angles θ, when the monopole's length is small (Fig. 9(a)), and we observe a slight difference between them for the longer monopole's shoulder (Fig. 9(b)). Such difference exists because of the different edge condition.

8. CONCLUSIONS

The mode matching technique and the analytical regularization procedure is developed for the solution of canonical diffraction problem of axially-symmetric excitation of bi-cone, formed by the finite and semi-infinite shoulders. With these techniques the diffraction problem has been reduced to ISLAE of the second kind, the solution of which satisfies all the necessary conditions. These solutions can be obtained with given accuracy by means of reduction methods. The simple low frequency solution in an explicit form and the transition from the bi-cone to the conical monopole and the disc-cone scatterer were obtained.

Numerical solution is used for examination of the scattering characteristics of two widely used structures: the conical monopole and the disc-cone. The scattering characteristics have been analyzed in a wide frequency range and for different locations of the excited source. It is shown that if the source is located close to the conical vertex ($kr_0 < 1$), then the TEM-source's mode dominates for both structures. Moving the source away from the vertex ($r_0 > \lambda/4$) leads to effective excitation of higher waves, which influences the far fields distribution significantly. The radiation power dependences on different scatterer parameters are analyzed, and the resonance character of scattering in low frequency range $a_1 < \lambda/2$ is found. The main amplitude of the scattered power is found to decrease, and the wide-band scattering property becomes better when the bi-conical area is wider for both structures. These properties became more prominent for the disc-cone with $a_1 > 3\lambda/2$.

APPENDIX A.

Taking into account the representation of the kernel function in Equation (29), here we show the formulas for effective calculation of the elements of matrix operator in Equation (28b) as:

$$M'_-(z_n) = \frac{\cos(\pi z_n)\dfrac{\partial}{\partial z}P_{z_n-1/2}(-\cos\gamma_1)}{(z_n^2-1/4)P_{z_n-1/2}(-\cos\gamma_2)R_{z_n-1/2}(\cos\gamma_2)M_+(z_n)};$$

$$\left\{[M_-(\xi_n)]^{-1}\right\}' = \begin{cases} -2\pi^{-1}M_+(1/2)\ln\left(\operatorname{ctg}\dfrac{\gamma_1}{2}\operatorname{tg}\dfrac{\gamma_2}{2}\right), \quad \xi_n = \nu_1 = 1/2; \\ \dfrac{(\xi_n^2-1/4)P_{\xi_n-1/2}(-\cos\gamma_2)M_+(\xi_n)\dfrac{\partial}{\partial\xi}R_{\xi_n-1/2}(\cos\gamma_2)}{\cos(\pi\xi_n)P_{\xi-1/2}(-\cos\gamma_1)}, \xi_n = \nu_n, \;\; n > 1; \\ \dfrac{(\xi_n^2-1/4)R_{\xi_n-1/2}(\cos\gamma_2)M_+(\xi_n)\dfrac{\partial}{\partial\xi}P_{\xi_n-1/2}(-\cos\gamma_2)}{\cos(\pi\xi_n)P_{\xi_n-1/2}(-\cos\gamma_1)}, \xi_n = \mu_n, \;\; n = \overline{1,\infty}. \end{cases}$$

REFERENCES

1. Rostomyan, N., A. T. Ott, M. D. Blech, R. Brem, C. J. Eisner, and T. F. Eibert, "Balanced impulse radiating omnidirectional ultrawideband stacked biconical antenna," *IEEE Trans. on Antennas and Propagation*, Vol. 63, No. 1, 59–68, 2015.
2. Khorshidi, M. and E. Tahanian, "A new conical band-reject UWB antenna with uniform rejection and stable omnidirectional behavior," *Progress In Electromagnetics Research C*, Vol. 59, 31–40, 2015.
3. Gilbert, A. M. and L. Ryan, "Ultra-wideband biconical antenna with excellent gain and impedance matching," US Patent 20150280317 A1, Oct. 1, 2015.
4. Palud, S., F. Colombel, M. Himdi, and C. L. Meins, "A novel broadband eighth-wave conical antenna," *IEEE Transactions on Antennas and Propagation*, Vol. 56, No. 7, 2112–2116, Jul. 2008.

5. Amert, A. K. and K. W. Whites, "Miniaturization of the biconical antenna for ultrawideband applications," *IEEE Transactions on Antennas and Propagation*, Vol. 57, No. 12, 3728–3735, Dec. 2009.
6. Kudpik, R., N. Siripon, K. Meksamoot, and S. Kosulvit, "Design of a compact biconical antenna for UWB applications," *Proc. International Symposium on Intelligent Signal Processing and Communications Systems (ISPACS)*, 1–6, Chiang Mai, Thailand, Dec. 7–9, 2011.
7. Yeoh, W. S. and W. S. T. Rowe, "An UWB conical monopole for multi-service wireless application," *Antennas and Wireless Propagation Letters*," Vol. 14, 1085–1088, 2015.
8. Lodge, O. J., "Electric telegraphy," US Patent 609,154, Aug. 16, 1898.
9. Carter, P. S., "Wide band, short wave antenna and transmission line system," US Patent 2,181,870, Oct. 10, 1939.
10. Barrow, W. L., "Biconical electromagnetic horn," US Patent 2,602,894. Jul. 8, 1952.
11. Schelkunoff S. A., "Theory of antennas of arbitrary size and shape," *Proc. IRE*, Vol. 29, No. 9. 493–521, 1941.
12. Schelkunoff, S. A., "Principal and complementary waves in antennas," *Proc. IRE*, Vol. 34, 23–32, 1946.
13. Schelkunoff, S. A., "General theory of symmetric biconical antennas," *J. Appl. Phys.*, Vol. 22, No. 11, 1330–1332, 1951.
14. Smith, P. D. P., "The conical dipole of wide angle," *J. App. Phys.*, Vol. 19, No. 1, 11–13, 1948.
15. Tai, C. T., "On the theory of biconical antennas," *J. App. Phys.*, Vol. 19, No. 12, 1155–1160, 1948.
16. Hahn, R. and J. G. Fikioris, "Impedance and radiation pattern of antennas above flat discs," *IEEE Trans. on Antennas and Propagation*, Vol. 21, No. 1, 97–100, 1973.
17. Papas, C. H. and R. W. King, "Input impedance of wide-angle conical antennas fed by a coaxial line," *Poc. IRE*, Vol. 37, No. 11, 1269–1271, 1949.
18. Papas, C. H. and R. W. King, "Radiation from wide-angle conical antennas fed by a coaxial Line," *Proc. IRE*, Vol. 39, No. 1, 49–51, 1951.
19. Kadakia, D. R. and J. G. Fikioris,, "Monopole antenna above a hemisphere," *IEEE Trans. Antennas Propagation* , Vol. 19, No. 5, 687–690, 1971.
20. Bolle, D. M. and M. D. Morganstern, "Monopole and conic antennas on spherical vehicles," *IEEE Trans. on Antennas and Propagation*, Vol. 17, No. 4, 477–484, 1969.
21. Bevensee, R. M., *A Handbook of Conical Antennas and Scatterers*, Gordon and Breach, New York, 1973.
22. Kuryliak, D. B., "Biconical line with slots in an axially symmetric electromagnetic field," *Proc. International Conference on Direct and Inverse Problems of Electromagenetic and Acoustic Wave Theory*, 46–47, 1995.
23. Kuryliak, D. B. and Z. T. Nazarchuk, "One conical waveguide bifurcation problem," *Technical Report of Electromagnetic Theory, Institute of Electrical Engineers of Japan,* No. EMT9750, 5156, 1997.
24. Kuryliak, D. B., "Wave diffraction from bifurcation of the conical region," *Izvestiya Vuzov. Radioelectronika*, Vol. 41, No. 9, 13–22, 1998 (in Russian).
25. Goshin, G. G., *Electrodynamics Value Boundary Problems for Conical Regions*, Izdatelstvo Tomsk Univ., Tomsk, 1987 (in Russian).
26. Doroshenko, V. A. and V. F. Kravchenko, *Electromagnetic Waves Diffraction on Unclosed Conical Structures*, Fizmatlit, Moscow, 2009 (in Russian).
27. Mohammadi, A., F. Kaminski, V. Sandoghdar, and M. Agio, "Fluorescence enhancement with the optical (bi-)conical antenna," *J. Phys. Chem. C*, Vol. 114, No. 16, 7372–7377, 2010.
28. Helfenstein, P., A. Mustonen, T. Feurer, and S. Tsujino, "Collimated field emission beams from metal double-gate nanotip arrays optically excited via surface plasmon resonance," *Applied Physics Express*, Vol. 6, 114301, 2013.

29. Legenkiy, M. N. and A. Y. Butrym, "Method of mode matching in time domain," *Progress In Electromagnetics Research B*, Vol. 22, 257–283, 2010.
30. Tretyakov, O. A., "Mode basis method," *Radiotekhnika and Elektronika*, Vol. 31, No. 6, 1071–1082, 1986 (in Russian).
31. Shestopalov, V. P., A. A. Kirilenko, and S. A. Masalov, *Convolution-type Matrix Equations in the Theory of Diffraction*, Naukova Dumka, Kyiv, 1984 (in Russian).
32. Kuryliak, D. B. and Z. T. Nazarchuk, *Analytical-numerical Methods in the Theory of Wave Diffraction on Conical and Wedge-shaped Surfaces*, Naukova Dumka, Kyiv, 2006 (in Ukrainian).
33. Kuryliak, D. B. and Z. T. Nazarchuk, "Convolution type operators for wave diffraction by conical structures," *Radio Science*, Vol. 43, RS4S03, 2008.
34. Kuryliak, D. B., Z. T. Nazarchuk, and V. O. Lysechko, "Diffraction of a plane acoustic wave from a finite soft (rigid) cone in axial irradiation," *Open Journal of Acoustics*, Vol. 5, 193–206, 2015.
35. Kuryliak, D. B. and O. M. Sharabura, "Axisymmetric electromagnetic excitation of a metallic discone scatterer," *Telecommunications and Radio Engineering*, Vol. 74, No. 7, 563–576, 2015.
36. Gradshteyn, I. S. and I. M. Ryzhik, *Tables of Integrals, Series and Products,* Dover, New York, 1972.